Online Calculation of Melt Pool Cooling Rate with Automatic Background Correction

Elena Rodríguez Lois, Roberto Fernández Molanes, Carlos González-Val, Juan J. Rodríguez-Andina, José Fariña
Dept. of Electronic Technology, University of Vigo, Vigo, Spain. AIMEN Technology Center, Porriño, Spain.
elenrodriguez@alumnos.uvigo.es, {roberto.fernandez, carlos.gonzalez}@aimen.es, {jjrdguez, jfarina}@uvigo.es

Abstract—**This paper presents a generic method to process mid-wave infrared (MWIR) images in laser-based manufacturing processes. The background noise of the camera is used as a source of information for correcting different problems that affect MWIR cameras. The mean of the noise distribution is used to correct the background drift due to sensor heat-up, whereas the standard deviation is used to generate dynamic thresholds for subsequent algorithms. The proposed method is portable, robust, and independent of the background, scale, and optical and electronic aberrations of the camera. The method is validated in the calculation of melt pool cooling rate. Performance is tested in a real scenario using a Field Programmable System-on-Chip platform. Results show that the system is capable of sending to a remote computer MWIR images at 1,435 frames per second and cooling rate information at a rate of 10,680 samples per second.**

I. INTRODUCTION

Custodian [1] is a European research project devoted to improving laser-based manufacturing processes using new and disruptive technologies. Although laser-based processes are faster, consume less energy, and produce smaller thermally affected areas than more traditional methods (i.e., electric arc), the high energy concentration also produces large temperature gradients, which are related to defects in the microstructure of materials, like brittle structures [2]. The aim of the project is to develop effective monitoring and control systems to avoid these kinds of defects.

The first step to reach the project objectives is to properly monitor thermal gradients in the process, especially in the fused material, known as melt pool. For this task, mid-wave infrared (MWIR) cameras are used, since they have demonstrated to be more effective than visible [3] and near infrared (NIR) [4] cameras. MWIR spectral range (1-6μm) allows thermal information to be captured at the high temperatures of the laser process (800-1,400ºC), where most of the visible and laser radiation is filtered.

Previous works on MWIR laser image analysis are based on static algorithms, hand-crafted for the application and setup, so reproducing them implies a long and tedious process. Changes in process parameters, setup, or materials cause changes in the nature of the images, forcing the redesign of these algorithms. Moreover, MWIR cameras tend to modify their background level and analog gain due to internal heat-up. These errors occur while the process is running and are hard to solve with an initial calibration for the setup, even if done at the beginning of every process.

In order to solve these problems this paper proposes a generic methodology to process MWIR images. First, an algorithm to automatically correct the background level of the MWIR images is presented. Then, a method to generate dynamic thresholds that separate the melt pool area from the background is proposed to correct changes in sensor gain and setup differences. This segmented image is used to measure melt pool cooling rate in the processing direction, as a way to evaluate the overall thermal treatment that the material is suffering, which is relevant for the objectives of the Custodian project.

A challenging issue in monitoring laser-based processes is their fast dynamics, usually above 1kHz [5][6]. In order to comply with the high frame rate requirements, the system is designed to be easily implementable in hardware (FPGA). To validate the proposed methodology and evaluate the maximum performance that can be achieved with current technologies, a Cyclone V Field Programmable System-on-Chip (FPSoC) device from Intel FPGA is used to implement the proposed algorithm. Its performance is tested for different combinations of camera frame rate, different ways of implementing the algorithm in hardware, and different amounts of information being sent to a remote system.

The remainder of the paper is organized as follows. Section II summarizes previous works on melt pool image processing. The proposed methodology is introduced in Section III. Section IV describes the proposed FPSoC implementation. The experimental tests carried out with the FPSoC implementation and the obtained results are presented and discussed in Sections V and VI, respectively. Finally, Section VII concludes the paper.

II. PREVIOUS WORKS

CMOS visible and NIR cameras were traditionally used for melt pool size control. The control of melt pool width in a cladding process using visible and NIR CMOS cameras is

presented in [7] and [8]. To do so, a fixed threshold is used to binarize images and the dimensions of the resulting ellipse corresponding to the cladding area are measured. These works show that visible/NIR images do not provide any thermal information. However, they are still useful for measuring melt pool dimensions.

MWIR cameras are currently more used than visible / NIR ones. In [9], high-speed control of laser metal deposition (LMD) using uncooled MWIR cameras is reported. The controlled parameter is melt pool width, obtained after binarization with a constant threshold. The implementation of a closed-loop control system for cladding is presented in [10]. A dynamic threshold is used to reduce the fuzziness level of the image, erasing parts of the image (such as flashes) not to be considered as part of the melt pool. Although a dynamic threshold is used, it only changes in order to correct blurriness, not image heat-up, which is addressed in this paper. Finally, the implementation and validation of an adaptative controller based also on measuring melt pool width after binarization with a constant threshold is presented in [11].

It can be noticed that none of the aforementioned works implements background correction, and a dynamic threshold is only used in [10], but for a different purpose from the one in this paper.

III. PROPOSED METHOD

A. Infrared Images

Fig. 1 shows a typical sample infrared image from a laser process. In these images three types of areas with differentiated pixel distributions can be usually identified:
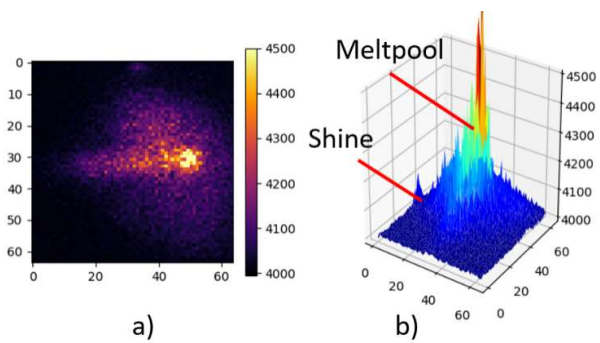

Fig. 1. 2D (a) and 3D (b) raw images from a laser welding process captured with a NIT Tachyon 16K camera. Scale is in digital level as produced by the sensor (nonlinearly related to temperature).

- Melt pool. These are the brightest areas in the image (yellow and red in Fig. 1a), which correspond to the point where the laser is being applied and to a liquid area of molten material.
- Thermally affected areas. These are areas with lower intensity level (purple in Fig. 1a), which correspond to parts of the material that are not molten but are still thermally affected by melt pool activity.

- Background, consisting of the rest of the image (dark areas in Fig. 1a), which contains no thermal information, and whose pixel values (black or close to that color) are mostly related to camera noise. When the laser is switched off all image belongs to the background distribution.

B. Background Correction

During image capture, infrared cameras tend to heat-up due to their internal components and the radiation coming from the process. This modifies both the image background level and the analog gain on the sensor converters. From the two, the background level modification has a more noticeable effect. It adds a constant offset to the whole image. The top plot in Fig. 2 shows results from an industrial laser welding process where this offset can be easily identified. The sudden changes are due to laser activation and deactivation during the process. However, the growing offset caused by heat-up can be clearly noticed, both with the laser on and off.
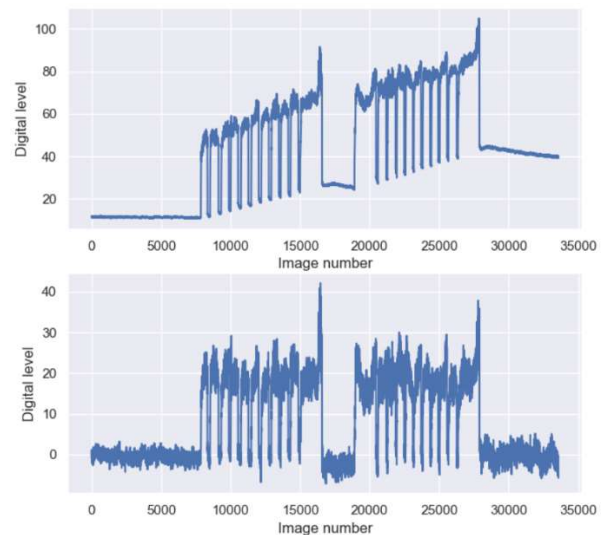

Fig. 2. Mean value of pixels in images from an infrared camera during a welding process in industrial environment without (top) and with (bottom) background correction. The images were captured at 1,000 fps.

This offset has a huge impact on the image processing algorithms (such as feature extraction) since they typically use static thresholds. If the threshold stays the same and the background level of pixels in the image changes, algorithms would extract wrong conclusions in subsequent steps. To reduce this negative effect, a background level calibration is usually applied before the process starts but, if the process lasts for more than a few seconds, the offset effect cannot be avoided. Another possible solution to mitigate this effect is to use a water-cooling refrigeration system. However, a great portion of the heating problem is generated at sensor level (in the pixel sensitive area and the analog-to-digital converters), for which refrigeration is just a partial solution.

In order to solve this problem, the following method for automatic correction of background offset is proposed:

- Automatic selection of background pixels. Assuming the background pixel distribution does not vary abruptly, the pixel values that fit into the background distribution are identified by comparing their value with the mean and standard deviation of background pixel distribution in previous images as follows. A pixel is selected as background if:

$$pix < \overline{bkg} + 3 \cdot \sigma(bkg) \qquad (1)$$

where pix is the pixel value, and $\overline{bkg}$ and $\sigma(bkg)$ are the mean and standard deviation, respectively, of the background pixels in the previous image. The factor 3 ensures pixels are inside the distribution (selection of 99.7% of values in a normal distribution, but it works for other distributions as well).

- Creation of a mask with the location of background pixels. An example is shown in Fig. 3a.
- Erosion of the mask to eliminate some pixels that, although fitting into the background distribution (Eq. (1)) do not belong to the background but to thermally affected areas. The result of eroding background in the mask of Fig. 3a is shown in Fig. 3b.
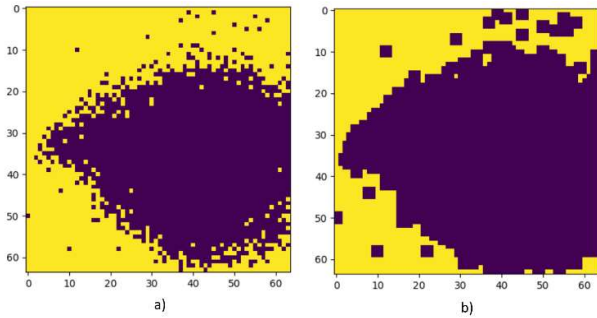- Background offset correction, by subtracting from all pixel values the mean value of background pixels.

Fig. 3. Initial background pixel selection mask (a) and final mask after a 3x3 erosion (b) of the image in Fig. 1. Yellow pixels represent background.

The result of this process, when applied to the dataset in Fig. 2a, is shown in Fig. 2b, where it can be clearly noticed that heat-up offset is completely removed.

The proposed automatic selection of background pixels provides additional advantages with respect to the easier solution of selecting certain fixed areas (blocks of pixels) as background. For instance, it prevents reflections and shines resulting in individual pixels with high value (that appear randomly anywhere in the image, as shown in Fig. 1b) from being used in background mean value calculations. It also avoids the need for somehow selecting those pixels (e.g., by human intervention), making the system easier to use and less prone to errors (i.e. the human operator may forget to set-up these pixels or may select pixels from the melt pool or thermally affected areas).

C. Cooling Rate Measurement

As stated in Section I, measuring the melt pool cooling rate is a key issue in the Custodian project this paper derives from. The proposed measurement method consists of calculating the slope of the line between the hottest point of the melt pool and that at the end of the thermally affected area in the processing direction, i.e., along the line through which the laser is being applied. The procedure to be followed with this purpose is (see Fig. 4):

- Image processing:
  o Correct offset background as explained in Section III-B.
  o Apply a 3x3 mean filter to soften the melt pool image, having a maximum more stable in time.
  o Create a dynamic threshold based on standard deviation. A pixel is considered cold when its value is below $4 \cdot \sigma(bkg)$ and hot when it is above it. Using a dynamic threshold based on background noise compensates for changes in the sensor analog gain mentioned in section III-B and is more robust than a constant threshold.
  o Segment the image using the previous dynamic threshold. Values below the threshold (cold pixels) are set to zero and above are not modified. The resulting image is shown in Fig. 4a.
- Obtain a 2D profile from the 3D segmented image, intersecting a vertical plane that contains the hottest point on the image and the processing direction. The resulting profile extracted from Fig. 4a is shown in Fig. 4b.
- Identification of the hottest point of the profile (and melt pool) as the one corresponding to the pixel with the highest value.
- Identification of the end of the thermally affected area as the transition point to cold values.
- Calculation of the slope of the line connecting the hottest point and that at the end of the thermally affected area, as shown in Fig. 4b.
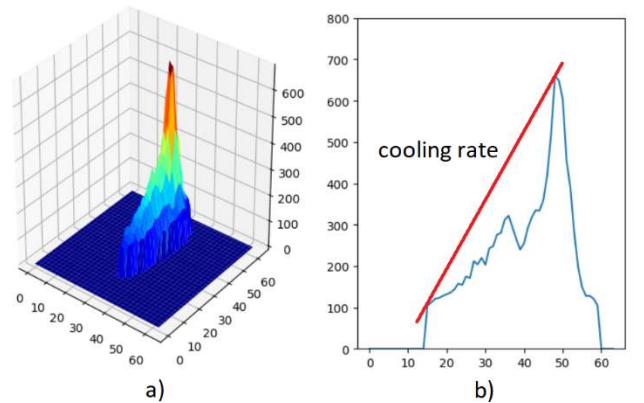

Fig. 4. 3D representation of image in Fig. 1 after image processing (a) and melt pool profile and cooling rate measurement extracted from it (b). Scales in digital level as produced by the sensor.

IV. FPSoC Implementation

This section describes the FPSoC implementation of the proposed cooling rate calculation method.

A. Background Analyzer

To carry out the proposed background offset correction, a background analyzer block, depicted in Fig. 5, has been designed. This block calculates the mean value and standard deviation of the background pixels, later used in background correction.
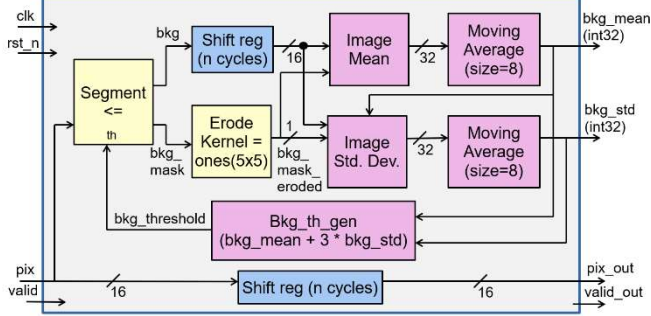

Fig. 5. Background analyzer block.

To identify background pixels, the raw image from the camera (pix signal in Fig. 5) is segmented using a (dynamic) threshold (bkg_threshold signal in Fig. 5). The Segment block generates the background mask (1 if the pixel value is below the threshold, 0 otherwise) as well as a version of the image delayed the exact number of cycles required to come out of the block synchronized with the mask.

After background pixels identification, the background mask is eroded. The original image (bkg in Fig. 5) is delayed for as long as required by the erosion operation. The original image and the background mask are sent to the blocks responsible to compute mean and standard deviation values. These blocks only use background pixels (those with mask value 1) to do their calculations, i.e., only the background pixels are used in the calculation of mean and standard deviation. To make these values more stable, they are filtered using moving average blocks with depth 8. When processing of each image is finished, the dynamic threshold is recalculated as the mean value plus 3 times the standard deviation and then used to segment the next image.

B. Background Correction and Cooling Rate Measurement

Background correction and cooling rate measurement are carried out by a melt pool image processing block, depicted in Fig. 6, based on the background analyzer block.

This block first removes background offset by subtracting the mean background value from the pixels in the raw image (pix_sync_delayed in Fig. 6). Then the operations required for cooling rate calculation, mean filter and segmentation are performed. Afterwards, a profiler generates a profile like the one in Fig. 4b. With this information, the cooling rate is calculated in the cooling rate calculator block, which identifies in the profile the hottest point and that at the end of the thermally affected area and calculates the slope of the line connecting them. The output of this block is generated in the format binary value/pixel, which can be easily translated (e.g., in software) into º/mm or º/s if required.
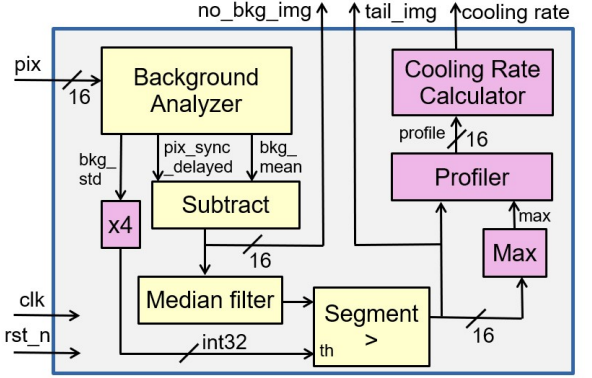

Fig. 6. Melt pool image processing block.

C. Full FPSoC System

FPSoC systems contain a Hard Processing System (HPS) including high-performance processors and FPGA logic in the same chip [12]. They are very suitable platforms for custom high-performance image processing applications, because the workload can be distributed between both parts (hardware and software) of the chip. The time-consuming image processing tasks can be implemented in the FPGA at high speed while high-level no time-critical tasks, such as communications and configuration, can be easily implemented in the processor. Fig. 7 shows the full block diagram of the FPSoC system for testing the cooling rate measurement algorithm.
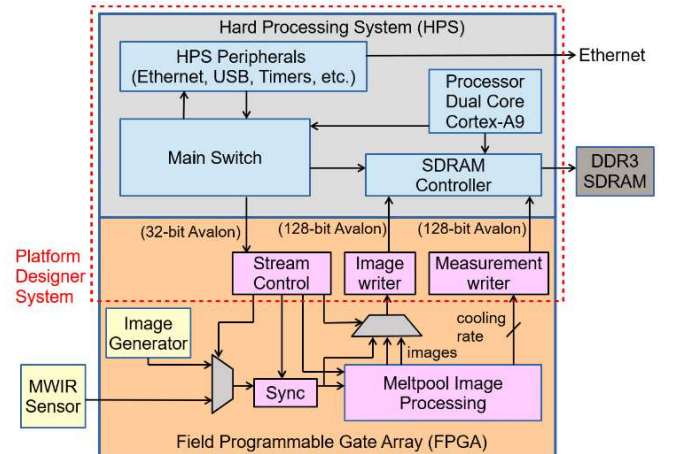

Fig. 7. Proposed FPSoC cooling rate calculation system.

The melt pool image processing block can process images from two sources: an external sensor (camera) or an internal image generator. Image writer and measurement

writer allow images and cooling rates, respectively, to be directly written from the FPGA into processor memory. The whole FPGA hardware is pipelined and can process images in real time at a rate of one pixel per clock cycle. This is the rate at which the cameras provide the images so no image will be lost, and real time control in the FPGA can be implemented at the same rate images are captured.

In the processor, a Python 3.6 server uses a driver to read images and/or cooling rates from memory and can send them to a remote computer using ZeroMQ library.

V. EXPERIMENTAL SETUP

A. Hardware and Programming Tools

To test the proposed cooling rate measurement method the system in Fig. 7 has been implemented in a Terasic DE0-nano-SoC board, featuring an Intel FPGA Cyclone V 5CSEMA4U23C6N and a dual-core ARM Cortex-A9 processor in the HPS. The board has 1GB DDR4 memory shared between the HPS and the FPGA. Tests have been carried out running Angstrom OS 2016.12 in the processor.

All functional blocks described in previous sections have been individually validated in separate projects to reduce errors during the integration phase. These projects have been also used to determine resource usage and maximum operating frequency of each component alone. All projects have been compiled using Intel Quartus Prime 18.1 Lite Edition with default compilation settings (balanced mode). Maximum frequency has been obtained from the timing analyzer included in Quartus.

B. Frame Rate Experiments

To test system performance, a set of frame rate measurements were carried out while images and/or cooling rate values were sent at maximum speed to a remote computer through a 100Mb/s Ethernet network.

To simplify these tests, 64x64 pixel images (similar to the one in Fig. 1) were generated with the image generator block instead of using a real camera, for which a real laser process would have been needed. FPGA frequency was set to 100MHz, because several commercial camera sensors work at frequencies slightly below this value. During the tests, two different hardware frame rates (denoted as FPGA fps) were used:

- 3,000 fps, corresponding to image streaming similar to that from a real camera. It is used to test the system under realistic conditions.
- 24,390 fps, corresponding to the maximum frame rate achievable with 64x64 pixel images with only three clock cycles between them and FPGA operating frequency 100MHz. It is used to test the board limits.

For each hardware frame rate, several software frame rates have been measured: frame rate in the HPS when just reading from hardware (HPS fps read), when reading from hardware and sending to computer (HPS fps read+send), and frame rate in the remote computer (PC fps). In this way, performance loss in the FPGA-HPS and HPS-computer connections can be evaluated. The following setups have been considered:

- IMG: images are read from hardware by HPS and directly sent to the computer, without any processing.
- FCR: cooling rates are read from hardware by HPS and directly sent to the computer. Images are not read from hardware by HPS.
- HCR: images are read from hardware by HPS and cooling rates are calculated in HPS. Images are not sent to the remote computer.
- PCR: HPS reads only images from hardware and sends them to the computer, which calculates cooling rates from them.

VI. EXPERIMENTAL RESULTS

A. Resource Usage

Resource usage and maximum operating frequency of the different blocks implemented, and the full system are listed on Table I. Despite the complexity of the image processing, the full system uses a relatively small percentage (around 40%) of available FPGA resources, leaving room for extensions and improvements. This low resource usage is due in part to the pipelined design, which allows pixels to be processed as they are received, without the need for intermediate memories. Regarding maximum operating frequency, it is higher than 100MHz for all components and the full system, making it compatible with most sensors/cameras in the market.

TABLE I. FPGA RESOURCE USAGE AND MAXIMUM FREQUENCY

Component	Resource usage			Max f.
	ALMs	M10K blocks	DSP blocks	(MHz)
Segment	14 (<1%)	0 (0%)	0 (0%)	285.70
Shift register	33 (<1%)	0 (0%)	0 (0%)	717.36
Erode	235 (1%)	1 (<1%)	0 (0%)	109.58
Image mean	483 (3%)	0 (0%)	0 (0%)	152.80
Image std. deviation	1,252 (8%)	2 (1%)	9 (11%)	131.29
Moving average	108 (<1%)	0 (0%)	0 (0%)	233.54
Bkg_th_gen	67 (<1%)	0 (0%)	1 (1%)	202.18
Background analyzer	2,664 (17%)	11 (4%)	11 (13%)	105.79
Mean filter	727 (5%)	8 (3%)	0 (0%)	126.86
Max	73 (<1%)	0 (0%)	0 (0%)	228.94
Profiler	62 (<1%)	0 (0%)	0 (0%)	276.17
Cooling rate calc.	525 (3%)	1 (<1%)	6 (7%)	137.04
Melt pool image proc.	3,731 (23%)	28 (10%)	17 (20%)	108.84
Measurement writer	51 (<1%)	0 (0%)	0 (0%)	215.66
Image writer	205 (<1%)	0 (0%)	0 (0%)	162.36
Image generator	194 (<1%)	32 (12%)	0 (0%)	-
Full system	6,064 (38%)	110 (41%)	17 (20%)	-

B. Frame Rate Analysis

Results regarding frame rate are summarized in Table II. The system is capable of sending images through the network (IMG data on Table II) at a maximum rate of 1,435 fps. With regard to the cooling rate, the maximum frame rate in HPS (FCR data on Table II) without sending images is 24,370 fps (close to the hardware fps), enabling embedded control by the processor at that rate. If cooling rate is read from the FPGA and directly sent to a remote computer 10,680 fps can be achieved, well above the few kHz required by the dynamics of laser processes. This means monitoring or control from a computer are also possible with this scheme. If the FPGA is used only to capture images and image processing is carried out in the HPS (HCR data on Table II) or the computer (PCR data on Table II), up to 8.5 and 227 fps can be achieved, respectively. These figures are much lower than those required by the application (in the order of thousands of fps) and justify the use of a full FPGA implementation of the image processing instead of a hybrid solution where HPS or the computer are in charge of part of the processing. Since full computer or embedded processor implementations are slower than the hybrid one, these options are also discarded, leaving the FPGA as the only platform capable of processing the algorithm with the required performance.

TABLE II. FRAME RATE ANALYSIS (FPS)

	FPGA fps = 3,000			FPGA fps = 24,390		
	HPS (read)	HPS (read+send)	PC	HPS (read)	HPS (read+send)	PC
IMG	3,000	2,995	1,435	9,200	5,770	1,435
FCR	3,000	3,000	3,000	24,370	10,695	10,680
HCR	8.5	8.5	8.5	8.5	8.5	8.5
PCR	3,000	3,000	227	9,100	8,600	227

VII. CONCLUSIONS

In this paper, a new method for processing images from MWIR cameras and determine the cooling rate of the melt pool in laser-based applications has been presented and validated. The method is robust, independent of the background differences due to setup and thermal heat-up of the sensor, and can be applied automatically, without any parameterization. The hardware implementation of the method allows the high frame rate required by laser-based industrial applications to be achieved.

The method has been validated in practice through an implementation in a low-cost DE0-nano-SoC board, including an FPSoC device that combines an FPGA fabric and a processor in the same chip. Experimental results show that the proposed hardware solution can work in real time at 100MHz, i.e., above the operating frequency of several commercial MWIR sensors. Performance tests with 64x64 pixel images show that the maximum frame rate that can be achieved in hardware is as high as 24,370 fps. Images can be sent to a remote computer at up to 1,435 fps, and cooling rate data at up to 10,680 fps. It can be concluded that the proposed solution is very suitable for the target industrial application.

REFERENCES

[1] Custodian project. [Online]. Available: http://www.shapeyourlaser.eu [Accessed: 13 June 2019].

[2] J. Svenungsson, I. Choquet, and A. F. H. Kaplan. "Laser welding process – A review of keyhole welding modelling," *Physics Procedia*, vol. 78, pp. 182-191, 2015.

[3] J. Rodríguez-Araújo, A. García-Díaz, V. Panadeiro, and C. Knaak, "Uncooled MWIR PbSe technology outperforms CMOS in RT closed-loop control and monitoring of laser processing," in *Proc. Applied Industrial Optics: Spectroscopy, Imaging and Metrology*, 2017, paper ATh2A.2.

[4] C. Knaak, U. Thombansen, O. Abels, and M. Kröger, "Machine learning as a CIRP comparative tool to determine relevance of signal features in laser welding," *Procedia CIRP*, pp. 623-627, 2018.

[5] V. V. Semak, J. A. Hopkins, M. H. McCay, and T. D. McCay, "Melt pool dynamics during laser welding," *Journal of Physics D: Applied Physics*, vol. 28, no. 12, p. 2443, Dec. 1995.

[6] R. Fabbro, S. Slimani, I. Doudet, F. Coste, and F. Briand, "Experimental study of the dynamical coupling between the induced vapour plume and the melt pool for Nd–Yag CW laser welding," *Journal of Physics D: Applied physics*, vol.39, no. 2, p. 394, Jan. 2006.

[7] S. Moralejo, X. Penaranda, S. Nieto, A. Barrios, A. Arrizubieta, I. Tabernero, and J. Figueras, "A feedforward controller for tuning laser cladding melt pool geometry in real time," *The International Journal of Advanced Manufacturing Technology,* vol. 89, no. 1-4, pp. 821-831, Mar. 2017.

[8] J. T. Hofman, B. Pathiraj, J. van Dijk, D.F. de Lange, and J. Meijer, "A camera based feedback control strategy for the laser cladding process," *Journal of Materials Processing Technology*, vol. 212, no. 11, pp. 2455-2462, Nov. 2012.

[9] V. Panadeiro-Castro, J. Rodríguez-Araújo, A García-Díaz, and G. Vergara, "Medium wavelength infrared (MWIR) imaging for high speed control of laser metal deposition (LMD)," *Lasers in Engineering*, vol. 39, no. 1-2, pp. 67-75, 2018.

[10] M. Asselin, E. Toyserkani, M. Iravani-Tabrizipour, and A. Khajepour, "Development of trinocular CCD-based optical detector for real-time monitoring of laser cladding," in *Proc. IEEE Int. Conf. Mechatronics and Automation*, 2005, vol. 3, pp. 1190-1196.

[11] J. Rodriguez-Araújo, J. J. Rodríguez-Andina, J. Farina, F. Vidal, J. L. Mato, and M. Á. Montealegre, "Industrial laser cladding systems: FPGA-based adaptive control," *IEEE Industrial Electronics Mag.*, vol. 6, no. 4, pp. 35-46, Dec. 2012.

[12] R. Fernández-Molanes, J. J. Rodriguez-Andina, and J. Farina, "Performance characterization and design guidelines for efficient processor-FPGA communication in FPSoC devices," *IEEE Trans. Ind. Electronics*, vol. 65, no. 5, pp. 4368-4377, May 2018.